

FortEPiaNO technical notes

S. Gariazzo,^{1,*} P.F. de Salas,^{2,†} and S. Pastor^{1,‡}

¹*Instituto de Física Corpuscular (CSIC-Universitat de València), Valencia, Spain*

²*The Oskar Klein Centre for Cosmoparticle Physics,*

Department of Physics, Stockholm University, SE-106 91 Stockholm, Sweden

We present here the main features of our code, **FORTRAN-Evolved Primordial Neutrino Oscillations** (**FortEPiaNO**) [1]. The code is publicly available at the url https://bitbucket.org/ahp_cosmo/fortepiano_public.

I. EQUATIONS

FortEPiaNO can compute oscillations with up to six neutrinos in the early universe. Neutrinos, including the sterile ones, are always treated as ultra-relativistic particles, which is a good approximation if the neutrino masses do not exceed $\mathcal{O}(\text{a few keV})$, i.e. neutrinos are still fully relativistic at decoupling. For larger masses, neutrinos may start to become non-relativistic before decoupling, and in that case one should take into account the effect of the mass.

The code computes the evolution of the $N \times N$ neutrino density matrix [2–5]

$$\varrho(x, y) = \begin{pmatrix} \varrho_{ee} & \varrho_{e\mu} & \varrho_{e\tau} & \varrho_{es_1} & \cdots \\ \varrho_{\mu e} & \varrho_{\mu\mu} & \varrho_{\mu\tau} & \varrho_{\mu s_1} & \\ \varrho_{\tau e} & \varrho_{\tau\mu} & \varrho_{\tau\tau} & \varrho_{\tau s_1} & \\ \varrho_{s_1 e} & \varrho_{s_1\mu} & \varrho_{s_1\tau} & \varrho_{s_1 s_1} & \\ \vdots & & & & \ddots \end{pmatrix}, \quad (1)$$

which is the same for neutrinos and antineutrinos, in terms of the comoving coordinates $x \equiv m_e a$, $y \equiv p a$, $z \equiv T_\gamma a$ and $w \equiv T_\nu a$. The momentum dependence of the density matrix ϱ is taken into account using a discrete grid of momenta, as described in section IV.

When using N neutrinos, the mixing matrix is defined as

$$U = R^{(N-1)N} \dots R^{1N} R^{(N-2)(N-1)} \dots R^{1(N-1)} \dots R^{34} R^{24} R^{14} R^{23} R^{13} R^{12}, \quad (2)$$

following and extending the convention presented in Eq. (12) of [6], where each R^{ij} is a real rotation matrix described by the angle θ_{ij} , containing $\cos \theta_{ij}$ in the diagonal elements ii and jj , 1 in the remaining diagonal elements, $\sin \theta_{ij}$ ($-\sin \theta_{ij}$) in the off-diagonal element ij (ji) and zero otherwise:

$$[R^{ij}]_{rs} = \delta_{rs} + (\cos \theta_{ij} - 1)(\delta_{ri}\delta_{sj} + \delta_{rj}\delta_{si}) + \sin \theta_{ij}(\delta_{ri}\delta_{sj} - \delta_{rj}\delta_{si}). \quad (3)$$

It enters the calculation of the rotated mass matrix $\mathbb{M}_F = U \mathbb{M} U^\dagger$, where the diagonal mass matrix is $\mathbb{M} = \text{diag}(m_1^2, \dots, m_N^2)$. Other matrices that we need to define are

$$\mathbb{E}_\ell = \text{diag}(\rho_e, \rho_\mu, 0, \dots), \quad \mathbb{P}_\ell = \text{diag}(P_e, P_\mu, 0, \dots), \quad \mathbb{E}_\nu = S_a \frac{1}{\pi^2} \left(\int dy y^3 \varrho \right) S_a \quad \text{with } S_a = \text{diag}(1, 1, 1, 0, \dots), \quad (4)$$

while the interaction matrices used in the collision terms, presented in section II, are

$$G^L = \text{diag}(g_L, \tilde{g}_L, \tilde{g}_L, 0, \dots), \quad G^R = \text{diag}(g_R, g_R, g_R, 0, \dots), \quad (5)$$

where $g_L = \sin^2 \theta_W + 1/2$, $\tilde{g}_L = \sin^2 \theta_W - 1/2$, $g_R = \sin^2 \theta_W$, and θ_W is the weak mixing angle. It is easy to see from the definitions of Eqs. (51) and (52) that the collision terms vanish when considering the interactions corresponding only to sterile neutrinos. When more than one sterile neutrino is considered, the damping terms between the different sterile neutrinos are therefore set to zero.

* gariazzo@ific.uv.es

† pablo.fernandez@fysik.su.se

‡ pastor@ific.uv.es

The definitions of comoving energy density and pressure, which can be combined to obtain the comoving entropy density, are written as:

$$\rho_i = g_i \int \frac{dp}{2\pi^2} p^2 E_p \frac{1}{e^{E_p/z} \pm 1}, \quad (6)$$

$$P = g_i \int \frac{dp}{2\pi^2} \frac{p^4}{3E_p} \frac{1}{e^{E_p/z} \pm 1}, \quad (7)$$

$$s = \frac{\rho + P}{z}, \quad (8)$$

where the $+$ ($-$) applies for fermions (bosons), i denotes the species, which has g_i degrees of freedoms, p is the comoving momentum, $E_p = \sqrt{p^2 + m_i^2}$, being m_i the comoving mass of the particle, and z must be substituted with w in the case of neutrinos.

To take into account finite temperature QED (FTQED) corrections [5, 7, 8], we have to modify the total pressure and energy density of the fluid:

$$P = \sum_{i=\gamma, \nu_i, e, \mu} P_i + \delta P(x, z), \quad (9)$$

$$\rho = \sum_{i=\gamma, \nu_i, e, \mu} \rho_i + \delta \rho(x, z), \quad (10)$$

where δP and $\delta \rho$ are contributions that can be computed using FTQED. It is convenient to define them in terms of the following functions:

$$J_a(r) = \frac{1}{\pi^2} \int_0^\infty du u^a \frac{\exp(\sqrt{u^2 + r^2})}{\left[\exp(\sqrt{u^2 + r^2}) + 1 \right]^2}, \quad (11)$$

$$K_a(r) = \frac{1}{\pi^2} \int_0^\infty du \frac{u^a}{\sqrt{u^2 + r^2}} \frac{1}{\exp(\sqrt{u^2 + r^2}) + 1}. \quad (12)$$

Let us also define for convenience:

$$\mathcal{N}_p = \frac{2}{e^{E_p/z} + 1}, \quad (13)$$

$$\partial_x \mathcal{N}_p = -\frac{x e^{E_p/z} \mathcal{N}_p^2}{2z E_p}, \quad (14)$$

$$\partial_z \mathcal{N}_p = \frac{e^{E_p/z} E_p \mathcal{N}_p^2}{2z^2}, \quad (15)$$

$$\partial_x \partial_z \mathcal{N}_p = \frac{x e^{E_p/z} \mathcal{N}_p^2}{2z^3} \left(1 - e^{E_p/z} \mathcal{N}_p + \frac{z}{E_p} \right). \quad (16)$$

The contributions δP and $\delta \rho$ can be expanded as a series of powers of the electron charge $e^2 = 4\pi\alpha$, where α is the fine structure constant. Taking into account the first orders of the expansion, and using $r = x/z$, for the pressure one has [8]

$$\delta P(x, z) = \delta P^{(2)}(x/z) + \delta P^{(2+\ln)}(x, z) + \delta P^{(3)}(x/z) + \dots, \quad (17)$$

$$\delta P^{(2)}(r) = -e^2 z^4 K_2 \left(\frac{1}{6} + \frac{K_2}{2} \right), \quad (18)$$

$$\delta P^{(2+\ln)}(x, z) = \frac{e^2 x^2}{16\pi^4} \iint_0^\infty dy dk \frac{y k}{E_y E_k} \ln \left| \frac{y+k}{y-k} \right| \mathcal{N}_y \mathcal{N}_k, \quad (19)$$

$$\delta P^{(3)}(r) = \frac{2e^3 z^4}{3\pi} \left(K_2 + \frac{r^2}{2} K_0 \right)^{3/2}, \quad (20)$$

while for the energy density the various terms are

$$\delta\rho(x, z) = \delta\rho^{(2)}(x/z) + \delta\rho^{(2+\ln)}(x, z) + \delta\rho^{(3)}(x/z) + \dots, \quad (21)$$

$$\delta\rho^{(2)}(r) = e^2 z^4 \left(\frac{K_2^2}{2} - \frac{K_2 + J_2}{6} - K_2 J_2 \right), \quad (22)$$

$$\delta\rho^{(2+\ln)}(x, z) = \frac{e^2 x^2}{16\pi^4} \iint_0^\infty dy dk \frac{y k}{E_y E_k} \ln \left| \frac{y+k}{y-k} \right| \mathcal{N}_y \left(2z \partial_z \mathcal{N}_k - \mathcal{N}_k \right), \quad (23)$$

$$\delta\rho^{(3)}(r) = \frac{e^3 z^4}{\pi} \left(K_2 + \frac{r^2}{2} K_0 \right)^{1/2} \left(J_2 + \frac{r^2}{2} J_0 \right). \quad (24)$$

In order to compute the evolution of the neutrino density matrix (1), we have to compute both the derivative of ϱ (as a function of the momentum) and of the comoving photon temperature z with respect to our time parameter x . The differential equations which the code solves are the following [2–5]:

$$\begin{aligned} \frac{d\varrho(y)}{dx} &= \sqrt{\frac{3m_{\text{Pl}}^2}{8\pi\rho}} \left\{ -i \frac{x^2}{m_e^3} \left[\frac{\mathbb{M}_F}{2y} - \frac{2\sqrt{2}G_F y m_e^6}{x^6} \left(\frac{\mathbb{E}_\ell + \mathbb{P}_\ell}{m_W^2} + \frac{4}{3} \frac{\mathbb{E}_\nu}{m_Z^2} \right), \varrho \right] + \frac{m_e^3}{x^4} \mathcal{I}(\varrho) \right\}, \\ \frac{dz}{dx} &= \frac{\sum_{\ell=e,\mu} \left[\frac{r_\ell^2}{r} J_2(r_\ell) \right] + G_1(r) - \frac{1}{2\pi^2 z^3} \int_0^\infty dy y^3 \sum_{\alpha=e}^{s_{N_s}} \frac{d\varrho_{\alpha\alpha}}{dx}}{\sum_{\ell=e,\mu} \left[r_\ell^2 J_2(r_\ell) + J_4(r_\ell) \right] + G_2(r) + \frac{2\pi^2}{15}}, \end{aligned} \quad (25)$$

where $r_\ell = m_\ell/m_e r$. The expressions for the G_1 and G_2 functions, which again take into account the FTQED corrections, are written as [5, 8]:

$$G_{1,2}(x, z) = G_{1,2}^{(2)}(x/z) + G_{1,2}^{(2+\ln)}(x, z) + G_{1,2}^{(3)}(x/z) + \dots, \quad (26)$$

$$G_a(r) = \frac{K_2'}{6} - K_2 K_2' + \frac{J_2'}{6} + K_2' J_2 + K_2 J_2', \quad (27)$$

$$G_1^{(2)}(r) = 2\pi\alpha \left[\frac{1}{r} \left(\frac{K_2}{3} + 2K_2^2 - \frac{J_2}{6} - K_2 J_2 \right) + G_a \right], \quad (28)$$

$$G_2^{(2)}(r) = -8\pi\alpha \left(\frac{K_2}{6} + \frac{J_2}{6} - \frac{1}{2} K_2^2 + K_2 J_2 \right) + 2\pi\alpha r G_a, \quad (29)$$

$$\begin{aligned} G_1^{(2+\ln)}(x, z) &= \frac{e^2 x}{16\pi^4 z^3} \iint_0^\infty dy dk \frac{y k}{E_y E_k} \ln \left| \frac{y+k}{y-k} \right| \left\{ -x \left[z \left(\partial_x \mathcal{N}_y \partial_z \mathcal{N}_k + \mathcal{N}_y \partial_x \partial_z \mathcal{N}_k \right) - \mathcal{N}_y \partial_x \mathcal{N}_k \right] \right. \\ &\quad \left. - \mathcal{N}_y \mathcal{N}_k - z \mathcal{N}_y \partial_z \mathcal{N}_k + \frac{x^2 (E_y^2 + E_k^2)}{2E_y^2 E_k^2} \left(2z \mathcal{N}_y \partial_z \mathcal{N}_k - \mathcal{N}_y \mathcal{N}_k \right) \right\}, \end{aligned} \quad (30)$$

$$G_2^{(2+\ln)}(x, z) = \frac{e^2 x^2}{16\pi^4 z^2} \iint_0^\infty dy dk \frac{y k}{E_y E_k} \ln \left| \frac{y+k}{y-k} \right| \partial_z \left(\mathcal{N}_y \partial_z \mathcal{N}_k \right), \quad (31)$$

$$G_b(r) = \sqrt{K_2 + r^2 \frac{K_0}{2}}, \quad (32)$$

$$G_c(r) = \frac{2J_2 + r^2 J_0}{2(2K_2 + r^2 K_0)}, \quad (33)$$

$$G_1^{(3)}(r) = \frac{e^3}{4\pi} G_b \left\{ \frac{1}{r} \left(2J_2 - 4K_2 \right) - 2J_2' - r^2 J_0' - r \left(2K_0 + J_0 \right) - G_c \left[r(K_0 - J_0) + K_2' \right] \right\}, \quad (34)$$

$$G_2^{(3)}(r) = \frac{e^3}{4\pi} G_b \left[G_c \left(2J_2 + r^2 J_0 \right) - \frac{2}{r} J_4' - r \left(3J_2' + r^2 J_0' \right) \right], \quad (35)$$

where the prime denotes derivative with respect to r and we dropped the explicit dependence on r in the expressions for the G functions. For the sake of computational speed, we calculate and store lists for all the terms of Eq. (25) which do not depend on the neutrino density matrix at the initialisation stage, and compute their values through interpolation during the real calculation. The same happens for the energy densities of charged leptons, for which performing an interpolation is much faster than computing an integral. The interpolation, however, can be disabled during compilation (see the README), with a $\lesssim 20\%$ increase of the running time.

In order to estimate the effective comoving neutrino temperature w , which is not needed for the calculation but useful to understand the final results, we use an equation similar to Eq. (25), but considering only relativistic electrons, i.e. fixing $r_e = 0$ in the equation.

The finite-temperature electromagnetic corrections are also taken into account in the calculation of the electron mass, used in the collision terms. The contribution to the electron mass, in comoving coordinates, is obtained as [5, 7, 8]:

$$\delta m_e^2(x, y, z) = \frac{2\pi\alpha z^2}{3} + \frac{4\alpha}{\pi} \int_0^\infty dk \frac{k^2}{E_k} \frac{1}{e^{E_k/z} + 1} - \frac{x^2\alpha}{\pi y} \int_0^\infty dk \frac{k}{E_k} \log \left| \frac{y+k}{y-k} \right| \mathcal{N}_k, \quad (36)$$

so that the comoving electron mass must be replaced using $x^2 \rightarrow x^2 + \delta m_e^2$. In the calculation of the collision integrals we ignore the log term that depends on y .

Finally, the effective number of degrees of freedom that the code returns in output is defined as:

$$N_{\text{eff}}^e = \frac{8}{7} \frac{\sum_i \rho_{\nu_i}}{\rho_\gamma} \quad \text{at early times,} \quad (37)$$

$$N_{\text{eff}}^l = \frac{8}{7} \left(\frac{11}{4} \right)^{4/3} \frac{\sum_i \rho_{\nu_i}}{\rho_\gamma} \quad \text{at late times,} \quad (38)$$

being ρ_γ the comoving energy density of photons and ρ_{ν_i} the one of the i -th neutrino.

II. COLLISION INTEGRALS

The full collision terms are defined by the sum of the contributions from neutrino–electron/positron scattering and e^\pm annihilation into neutrinos. We neglect other reactions, such as μ^\pm annihilation (which only affects at very early temperatures when everything is in equilibrium) and neutrino–neutrino scattering. We therefore have [2]

$$\mathcal{I}[\varrho(y)] = \frac{G_F^2}{(2\pi)^3 y^2} (\mathcal{I}_{\text{sc}}^u + \mathcal{I}_{\text{ann}}^u), \quad (39)$$

$$\mathcal{I}_{\text{sc}}^u = \int dy_2 dy_3 \frac{y_2}{E_2} \frac{y_4}{E_4} \quad (40)$$

$$\left\{ (\Pi_2^s(y, y_4) + \Pi_2^s(y, y_2)) \left[F_{\text{sc}}^{LL}(\varrho^{(1)}, f_e^{(2)}, \varrho^{(3)}, f_e^{(4)}) + F_{\text{sc}}^{RR}(\varrho^{(1)}, f_e^{(2)}, \varrho^{(3)}, f_e^{(4)}) \right] \right. \\ \left. - 2(x^2 + \delta m_e^2) \Pi_1^s(y, y_3) \left[F_{\text{sc}}^{RL}(\varrho^{(1)}, f_e^{(2)}, \varrho^{(3)}, f_e^{(4)}) + F_{\text{sc}}^{LR}(\varrho^{(1)}, f_e^{(2)}, \varrho^{(3)}, f_e^{(4)}) \right] \right\},$$

$$\mathcal{I}_{\text{ann}}^u = \int dy_2 dy_4 \frac{y_3}{E_3} \frac{y_4}{E_4} \quad (41)$$

$$\left\{ \Pi_2^a(y, y_4) F_{\text{ann}}^{LL}(\varrho^{(1)}, \varrho^{(2)}, f_e^{(3)}, f_e^{(4)}) + \Pi_2^a(y, y_3) F_{\text{ann}}^{RR}(\varrho^{(1)}, \varrho^{(2)}, f_e^{(3)}, f_e^{(4)}) \right. \\ \left. + (x^2 + \delta m_e^2) \Pi_1^a(y, y_2) \left[F_{\text{ann}}^{RL}(\varrho^{(1)}, \varrho^{(2)}, f_e^{(3)}, f_e^{(4)}) + F_{\text{ann}}^{LR}(\varrho^{(1)}, \varrho^{(2)}, f_e^{(3)}, f_e^{(4)}) \right] \right\},$$

where $E_i^2 = \sqrt{x^2 + y_i^2 + \delta m_e^2}$ and

$$\Pi_1^s(y, y_3) = y y_3 D_1 + D_2(y, y_3, y_2, y_4), \quad (42)$$

$$\Pi_1^a(y, y_2) = y y_2 D_1 - D_2(y, y_2, y_3, y_4), \quad (43)$$

$$\Pi_2^s(y, y_2)/2 = y E_2 y_3 E_4 D_1 + D_3 - y E_2 D_2(y_3, y_4, y, y_2) - y_3 E_4 D_2(y, y_2, y_3, y_4), \quad (44)$$

$$\Pi_2^s(y, y_4)/2 = y E_2 y_3 E_4 D_1 + D_3 + E_2 y_3 D_2(y, y_4, y_2, y_3) + y E_4 D_2(y_2, y_3, y, y_4), \quad (45)$$

$$\Pi_2^a(y, y_3)/2 = y y_2 E_3 E_4 D_1 + D_3 + y E_3 D_2(y_2, y_4, y, y_3) + y_2 E_4 D_2(y, y_3, y_2, y_4), \quad (46)$$

$$\Pi_2^a(y, y_4)/2 = y y_2 E_3 E_4 D_1 + D_3 + y_2 E_3 D_2(y, y_4, y_2, y_3) + y E_4 D_2(y_2, y_3, y, y_4), \quad (47)$$

where the functions D_i have the following definitions [9]:

$$D_1(a, b, c, d) = \frac{16}{\pi} \int_0^\infty \frac{d\lambda}{\lambda^2} \prod_{i=a,b,c,d} \sin(\lambda i), \quad (48)$$

$$D_2(a, b, c, d) = -\frac{16}{\pi} \int_0^\infty \frac{d\lambda}{\lambda^4} \prod_{i=a,b} [\lambda i \cos(\lambda i) - \sin(\lambda i)] \prod_{j=c,d} \sin(\lambda j), \quad (49)$$

$$D_3(a, b, c, d) = \frac{16}{\pi} \int_0^\infty \frac{d\lambda}{\lambda^6} \prod_{i=a,b,c,d} [\lambda i \cos(\lambda i) - \sin(\lambda i)]. \quad (50)$$

The three functions can be written in a more efficient way for the calculation, since they can be solved analytically, see e.g. [10] for the complete expressions.

Finally, the functions that define the phase space factors in the collision terms are [2]:

$$F_{\text{sc}}^{ab}(\varrho^{(1)}, f_e^{(2)}, \varrho^{(3)}, f_e^{(4)}) = f_e^{(4)}(1 - f_e^{(2)}) \left[G^a \varrho^{(3)} G^b (1 - \varrho^{(1)}) + (1 - \varrho^{(1)}) G^b \varrho^{(3)} G^a \right] \\ - f_e^{(2)}(1 - f_e^{(4)}) \left[\varrho^{(1)} G^b (1 - \varrho^{(3)}) G^a + G^a (1 - \varrho^{(3)}) G^b \varrho^{(1)} \right], \quad (51)$$

$$F_{\text{ann}}^{ab}(\varrho^{(1)}, \varrho^{(2)}, f_e^{(3)}, f_e^{(4)}) = f_e^{(3)} f_e^{(4)} \left[G^a (1 - \varrho^{(2)}) G^b (1 - \varrho^{(1)}) + (1 - \varrho^{(1)}) G^b (1 - \varrho^{(2)}) G^a \right] \\ - (1 - f_e^{(3)})(1 - f_e^{(4)}) \left[G^a \varrho^{(2)} G^b \varrho^{(1)} + \varrho^{(1)} G^b \varrho^{(2)} G^a \right], \quad (52)$$

where $\varrho^{(i)} = \varrho(y_i)$ and $f_e^{(i)} = f_{\text{FD}}(y_i, z)$ represent the momentum distribution function of the various particles. The full expression for these functions should take into account the lepton asymmetry and distinguish the momentum distributions of leptons/neutrinos from those of antilepton/antineutrinos. Since we do not include lepton asymmetry, we just report the expressions without the heavier notation required to distinguish the various terms.

The code we use can compute the collision terms according to Eqs. (40) and (41), but the integrals are very expensive. For the non-diagonal terms of the collision matrix we therefore use the damping approximation, in the form

$$\mathcal{I}_{\alpha\beta}(\varrho) = -D_{\alpha\beta} \varrho_{\alpha\beta}, \quad (53)$$

for $\alpha \neq \beta$. The expressions for the coefficients $D_{\alpha\beta}$ depend on the elements considered. The coefficients were derived for example in [11], see also [12, 13], and can be written as

$$D_{e\mu}/F = D_{e\tau}/F = 15 + 8 \sin^4 \theta_W, \quad (54)$$

$$D_{\mu\tau}/F = 7 - 4 \sin^2 \theta_W + 8 \sin^4 \theta_W, \quad (55)$$

$$D_{es}/F = 29 + 12 \sin^2 \theta_W + 24 \sin^4 \theta_W, \quad (56)$$

$$D_{\mu s}/F = D_{\tau s}/F = 29 - 12 \sin^2 \theta_W + 24 \sin^4 \theta_W, \quad (57)$$

where $F = 7\pi^4 y^3/135$ is a common normalisation coefficient. In case more than one sterile state is considered, the terms $D_{s_i s_j}$ are always zero.

III. SOLVER AND INITIAL CONDITIONS

We solve the differential equations with the DLSODA routine from the ODEPACK[14] Fortran package [15, 16]. ODEPACK is a collection of solvers for the initial value problem for systems of ordinary differential equations. It includes methods to deal with stiff and non-stiff systems, and some of the provided subroutines automatically recognise which type of problem they are facing.

The specific solver we use, DLSODA, is a modification of the Double-precision Livermore Solver for Ordinary Differential Equations (DLSODE) which includes an automatic switching between stiff and non-stiff problems of the form $dy/dt = f(t, y)$. In the stiff case, it treats the Jacobian matrix df/dy as either a dense (full) or a banded matrix, and as either user-supplied or internally approximated by difference quotients. It uses Adams methods (predictor-corrector) in the non-stiff case, and Backward Differentiation Formula (BDF) methods (the Gear methods) in the stiff case. The linear systems that arise are solved by direct methods (LU factor/solve). For more details, see the original publications [15, 16].

The initial conditions for DLSODA are defined as follows. The initial time x_{in} is an input parameter of the code, and reasonable values would correspond to temperatures between a few hundreds and a few tens of MeV. The initial comoving photon temperature is computed evolving Eq. (25) from even earlier times ($z_0 = 1$ at $T_0 = 10 m_\mu$, $x_0 = m_e/T_0$) until x_{in} . The obtained value z_{in} is then considered as the temperature of equilibrium of the entire plasma. Concerning the neutrino density matrix at x_{in} , all off-diagonal elements and the diagonal ones for sterile neutrinos are fixed to zero, while the diagonal elements corresponding to active neutrinos are Fermi-Dirac distributions with a temperature z_{in} . For typical values that we use in the code, we have $z_{\text{in}} - 1 = 2.9 \times 10^{-4}$ for $x_{\text{in}} = 0.001$ (which we use for the 3+1 cases) or $z_{\text{in}} = 1.098$ for $x_{\text{in}} = 0.05$ (suitable for the three-neutrino case, see [2]).

IV. MOMENTUM GRID

In order to follow the evolution of Eq. (1), we discretise its dependence on y and evolve each of the momentum in x . One of the most interesting ways to make the code more precise and faster is related to the choice of the y_i . Discretising the momenta with a linear or logarithmic spacing works, but it is not the most efficient way to generate the grid. Inspired by one of the methods used in CLASS (see [17]), we deeply tested and finally considered a spacing based on the Gauss-Laguerre integration method. The crucial point of the calculation is to compute the energy density of neutrinos, given by

$$\rho_\alpha = \frac{1}{\pi^2} \int_0^\infty dy y^3 \varrho_{\alpha\alpha}(y), \quad (58)$$

where $\varrho_{\alpha\alpha}(y)$ will be close to a Fermi-Dirac distribution and in any case always exponentially suppressed. The Gauss-Laguerre quadrature (see e.g. [18]) is a method that is designed to optimise the solution of integrals of the type

$$I = \int_0^\infty dx y^\alpha e^{-y} f(y) \simeq \sum_i^N w_i^{(\alpha)} f(y_i), \quad (59)$$

where $f(y)$ is a generic function, y_i are the N roots of the Laguerre polynomial L_N of order N , and w_i are relative weights, which are obtained using

$$w_i^{(\alpha)} = \frac{y_i}{(N+1)^2 \left[L_{N+1}^{(\alpha)}(y_i) \right]^2}. \quad (60)$$

The weights can be computed for example using the `gaulag` routine from [18]. Since our momentum distribution function is not directly proportional to e^{-y} , we consider $f(x) = e^y \varrho_{\alpha\alpha}(y)$, in order to rescale the weights appropriately.

For the simple purpose of integrating the Fermi-Dirac distribution, very few points are typically required. CLASS, for example, uses order of ten points for integrating the neutrino distribution. In our case the non-thermal distortions must be computed accurately, and in particular when evolving the thermalisation of a sterile neutrino we need more precision on the small momenta. On the other hand, we do not want to compute the momentum distribution function at very high y , which gives a very small contribution to the total integral. We therefore use a truncated list of nodes y_i over which to compute the evolution of ϱ , selecting only the $N_y \leq N$ nodes for which $y_i < 20$. In this way we can increase the number of points at small y and the resolution on the thermalisation processes without having to compute a large number of points at high momentum. The number of points we can use is limited by the accuracy of the algorithm that computes the w_i . For the `gaulag` routine [18], our setup allows to reach $N_y \sim 50$ when $N \sim 350$. This number of momentum nodes is already large enough to reach a precision much better than one per mille on N_{eff} , which is the same we could obtain with a linear spacing of the points and $N_y = 100$ [2]. Since the evaluation of the collision integrals scales as N_y^2 and the number of derivatives in Eq. (25) scales with N_y , this ensures a significant gain. We further comment on this point in the next sections.

V. NUMERICAL CALCULATION OF 1D AND 2D INTEGRALS

Most of the processing time is spent to compute the collision integrals discussed in section II, which are two-dimensional integrals in the momentum. We compute the integrals using a two-dimensional version of the Gauss-Laguerre method, which has been tested to be precise enough,

$$\int_{x_1}^{x_N} \int_{y_1}^{y_M} dx dy f(x, y) = \sum_{i=1}^N \sum_{j=1}^M w_i w_j f_{ij}. \quad (61)$$

This works under the assumption that $f(x, y)$ is exponentially suppressed both in x and y . Such assumption is valid in our case, as the functions F_{ab} always contain products of momentum distribution functions, which are typically very close to the Fermi-Dirac. The only exception is the case of the additional neutrino, for which the distribution can be very different from the Fermi-Dirac, but in any case it is always exponentially suppressed, since the lowest momenta are always populated first and its momentum distribution can never exceed the one of standard neutrinos.

When using a linear/logarithmic spacing of points, instead we perform the integrals using a composite two-dimensional Newton-Cotes formula of order 1 [19]:

$$\int_{x_1}^{x_N} \int_{y_1}^{y_M} dx dy f(x, y) = \sum_{i=1}^{N-1} \sum_{j=1}^{M-1} (x_j - x_i)(y_j - y_i) \left[\frac{f_{ij} + f_{i+1,j} + f_{i,j+1} + f_{i+1,j+1}}{4} \right], \quad (62)$$

where we used the short notation $f_{i,j} = f(x_i, y_j)$, while i and j run over the grid of momenta we are using, which contains $N = M = N_y$ points for each dimension. This avoids us the need to interpolate the density matrix in points outside the momentum grid.

The integrals therefore require N_y^2 evaluations of the integrands at each evaluation: this means that reducing the value of N_y by a factor of two gives a factor four faster calculation of the integrals. The actual gain in the code is even larger, since the DLSODA algorithm needs to explore less combinations of variations in the $\varrho_{\alpha\beta}(y_l)$ for the different y_l in the momentum grid. Our goal is therefore to obtain with a coarse grid a result that is in reasonable agreement with the one obtained using a fine grid.

In order to obtain the maximum speed, we study the accuracy of each function that enters the code in comparison with the analytical results, were they can be obtained. The number of points and the integration methods adopted in all the integrals, for example, have been carefully studied to achieve a reasonable precision with a short computation time. For the two-dimensional integrals, the selected momentum grid fully defines the integration procedure, and the precision is always good when using a reasonable number of points. Depending on the function, we may adopt the Gauss-Laguerre, Newton-Cotes or Romberg integration [20] methods for the one-dimensional integrals. In particular, for the electron and muon energy densities and for most of the functions that enter the calculation of Eq. (25) we use a Gauss-Laguerre method on a dedicated grid of up to 110 points for the most complicated functions. In one single case, the $K'(r)$ function derived from Eq. (12), the result obtained with the Gauss-Laguerre method did not reach the requested precision and we decided to use a Romberg integration instead. Although this requires a longer computation time, it only affects the initialisation stage, as in the code we interpolate over the pre-computed values. The number of points and the interpolation range have also been studied in order to obtain sufficiently precise results for all the computations required in the code.

VI. PRECISION OF THE FINAL RESULTS

We have tested our code with the results available in the literature and verified the robustness of our findings against changes in the settings used in the calculations. In particular, we refer to the high-precision results in the three-neutrino case of [2], from which we have adopted all the equations.

Concerning the value of N_{eff} that we obtain using only active neutrinos, we verified that we can reach much better than per mille stability on $N_{\text{eff}} = 3.044$ using $N_y \geq 20$ points spaced with the Gauss-Laguerre method, if the tolerance for DLSODA[21] is 10^{-6} . This means that using $N_y = 50$ instead of $N_y = 20$ does not significantly alter the result. If we want to consider a linear or logarithmic spacing for the momentum grid, a minimum of 40 grid points must be employed in order to reach the same level of stability. Another possible setting that can give us a faster execution of the code is the precision used for DLSODA. We verified that once the tolerance for DLSODA is smaller than 10^{-5} , the results are already stable at a level much better than per mille (actually closer to the 0.1 per mille) with respect to the most precise case considered here ($N_y = 50$, tolerance 10^{-6}). Using a tolerance of 10^{-4} gives a value of N_{eff} which is stable at the level of few per mille, and still better than 1%.

If we repeat the same exercise in the 3+1 scheme, using $\Delta m_{41}^2 = 1.29 \text{ eV}^2$, $|U_{e4}|^2 = 0.012$ [22] and $|U_{\mu 4}|^2 = |U_{\tau 4}|^2 = 0$, we find similar conclusions. A tolerance of 10^{-5} gives results very close to those obtained with 10^{-6} , while any larger tolerance gives larger fluctuations depending on N_y . With 10^{-4} , the precision remains of the order of 0.5%, so it is still safe to compute the value of N_{eff} on a grid of active-sterile mixing parameters using this level of precision. With $N_y = 20$, a single run takes a few minutes on four cores, and the running time is not significantly affected by changes in the DLSODA tolerance. When more precision is required, however, the algorithm may have troubles in resolving some of the resonances, and in that case the run can take much longer because of the adaptive nature of the solver.

Another parameter that we tested is the initial value of x , x_{in} . Apart from fluctuations which are compatible with those obtained varying N_y , the result is stable against variations in $5 \times 10^{-4} \leq x_{\text{in}} \leq 5 \times 10^{-2}$. The largest values of

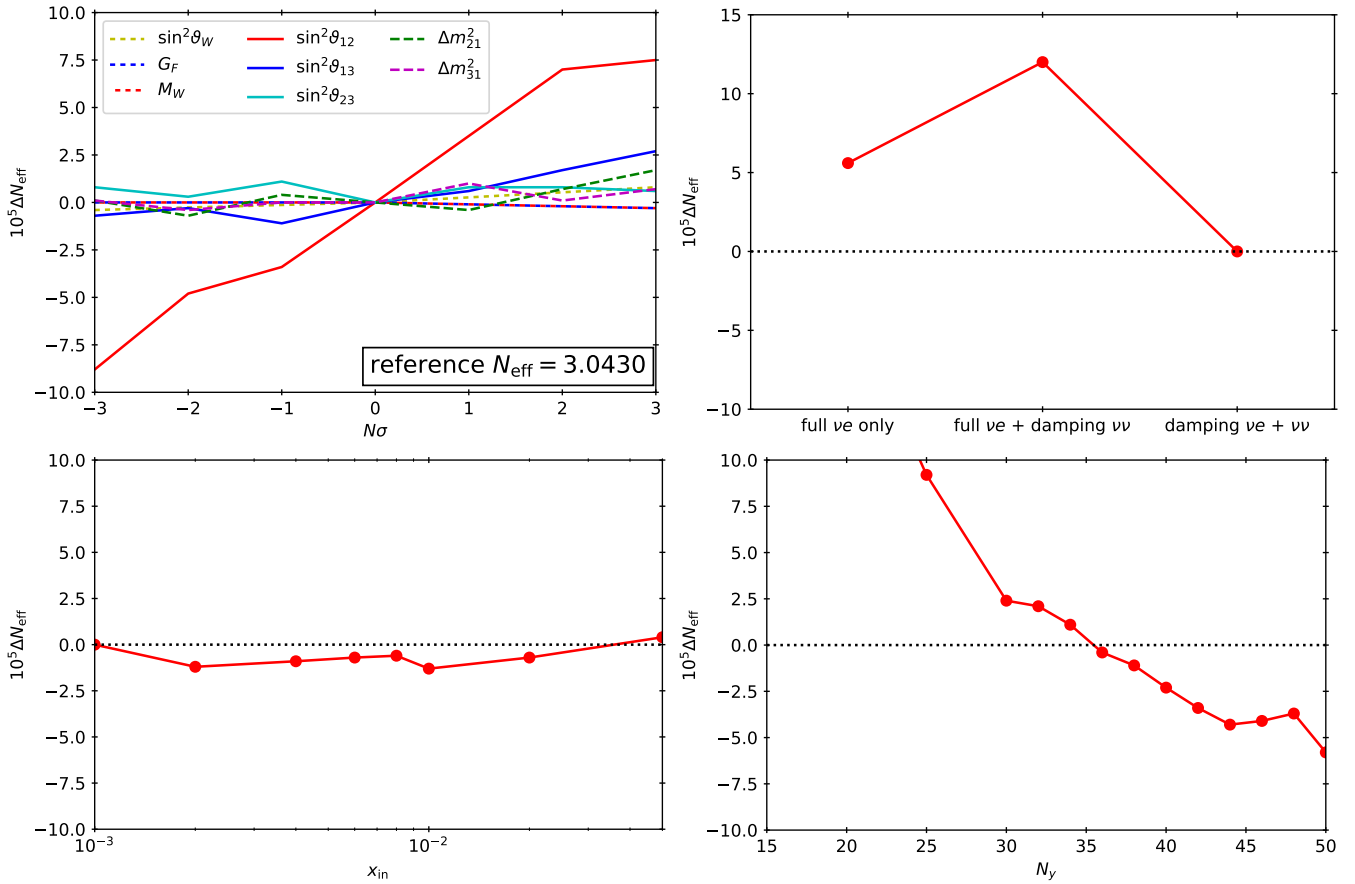


FIG. 1. Absolute variations of N_{eff} as a function of the physical parameters (upper left) or of some crucial numerical settings: the different contributions to the off-diagonal terms of the collision integrals (upper right), the initial value x_{in} (lower left), the number of nodes in the y grid (lower right).

x_{in} may be inappropriate for high values of Δm_{41}^2 , as it is important for the solver to start the evolution before the sterile state starts to oscillate significantly with the active ones. Smaller values, on the contrary, may create numerical problems in DLSODA due to the very small initial value $z_{\text{in}} - 1$, and are never really required for our purposes.

More details on the precision of numerical calculations and the dependence of N_{eff} on physical parameters (including Fermi constant, Weinberg angle, W boson mass and neutrino mixing parameters) are discussed in [23], considering the three-neutrino case only. We report here some of the main results, summarized in the various panels of Fig. 1. In order to study the accuracy of the numerical calculations as functions of the physical parameters, the tolerance for DLSODA has been set to 10^{-7} . Considering variations for the physical parameters in the allowed 3σ range (from [24] for the neutrino mixing parameters, from [25] for the weak interaction parameters), we see that the stability of N_{eff} is at the 10^{-4} level or better (upper left panel). A similar precision is obtained when changing the way the off-diagonal terms (upper right panel). Altering x_{in} (lower left panel), which controls the initial time in the code, only affects N_{eff} at the 10^{-5} level. More critical is the dependence on N_y (lower right panel), which controls the number and the position of the nodes of the momentum grid. Varying N_y between 25 and 50 only alters the final result at the 10^{-4} level, so that it is safe to quote our suggested number $N_{\text{eff}} = 3.0430$ when considering 3 neutrinos. An estimate of the theoretical and numerical uncertainty on this number is of order 10^{-4} .

ACKNOWLEDGMENTS

We thank J.J. Bennett and G. Buldgen for helping spotting some issue in the treatment of finite temperature corrections and for support in implementing the higher order correction terms.

This software is part of a project that has received funding from the European Union's Horizon 2020 research and

innovation programme, under the Marie Skłodowska-Curie grant agreement No 796941.

-
- [1] S. Gariazzo, P. F. de Salas, and S. Pastor, *Thermalisation of sterile neutrinos in the early Universe in the 3+1 scheme with full mixing matrix*, *JCAP* **07** (2019) 014, [[arXiv:1905.11290](#)].
 - [2] P. F. de Salas and S. Pastor, *Relic neutrino decoupling with flavour oscillations revisited*, *JCAP* **07** (2016) 051, [[arXiv:1606.06986](#)].
 - [3] A. Mirizzi, N. Saviano, G. Miele, and P. D. Serpico, *Light sterile neutrino production in the early universe with dynamical neutrino asymmetries*, *Phys.Rev.D* **86** (2012) 053009, [[arXiv:1206.1046](#)].
 - [4] N. Saviano, A. Mirizzi, O. Pisanti, P. D. Serpico, G. Mangano, and G. Miele, *Multi-momentum and multi-flavour active-sterile neutrino oscillations in the early universe: role of neutrino asymmetries and effects on nucleosynthesis*, *Phys.Rev.D* **87** (2013) 073006, [[arXiv:1302.1200](#)].
 - [5] G. Mangano, G. Miele, S. Pastor, and M. Peloso, *A Precision calculation of the effective number of cosmological neutrinos*, *Phys.Lett.B* **534** (2002) 8–16, [[astro-ph/0111408](#)].
 - [6] S. Gariazzo, C. Giunti, M. Laveder, Y. F. Li, and E. M. Zavatin, *Light sterile neutrinos*, *J.Phys.G* **43** (2016) 033001, [[arXiv:1507.08204](#)].
 - [7] N. Fornengo, C. Kim, and J. Song, *Finite temperature effects on the neutrino decoupling in the early universe*, *Phys.Rev.D* **56** (1997) 5123–5134, [[hep-ph/9702324](#)].
 - [8] J. J. Bennett, G. Buldgen, M. Drewes, and Y. Y. Wong, *Towards a precision calculation of the effective number of neutrinos N_{eff} in the Standard Model I: The QED equation of state*, [arXiv:1911.04504](#).
 - [9] A. Dolgov, S. Hansen, and D. Semikoz, *Nonequilibrium corrections to the spectra of massless neutrinos in the early universe*, *Nucl.Phys.B* **503** (1997) 426–444.
 - [10] D. N. Blaschke and V. Cirigliano, *Neutrino Quantum Kinetic Equations: The Collision Term*, *Phys.Rev.D* **94** (2016), no. 3 033009, [[arXiv:1605.09383](#)].
 - [11] B. H. McKellar and M. J. Thomson, *Oscillating doublet neutrinos in the early universe*, *Phys.Rev.D* **49** (1994) 2710–2728.
 - [12] K. Enqvist, K. Kainulainen, and M. J. Thomson, *Stringent cosmological bounds on inert neutrino mixing*, *Nucl.Phys.B* **373** (1992) 498–528.
 - [13] N. F. Bell, R. R. Volkas, and Y. Y. Y. Wong, *Relic neutrino asymmetry evolution from first principles*, *Phys.Rev.D* **59** (1999) 113001, [[hep-ph/9809363](#)].
 - [14] https://computation.llnl.gov/casc/odepack/odepack_home.html.
 - [15] A. Hindmarsh and L. L. Laboratory, *ODEPACK, a Systematized Collection of ODE Solvers*. Lawrence Livermore National Laboratory, 1982.
 - [16] K. Radhakrishnan and A. C. Hindmarsh, *Description and use of LSODE, the Livermore solver for ordinary differential equations*, .
 - [17] J. Lesgourgues and T. Tram, *The Cosmic Linear Anisotropy Solving System (CLASS) IV: efficient implementation of non-cold relics*, *JCAP* **09** (2011) 032, [[arXiv:1104.2935](#)].
 - [18] N. Kaiser, *Clustering in real space and in redshift space*, *Monthly Notices of the Royal Astronomical Society* **227** (jul, 1987) 1–21.
 - [19] “Newton-Cotes quadrature formula.” Encyclopedia of Mathematics.
http://www.encyclopediaofmath.org/index.php?title=Newton%E2%80%93Cotes_quadrature_formula&oldid=22842.
 - [20] W. Romberg, *Vereinfachte numerische integration*, *Norske Vid. Selsk. Forh.* **28** (1955) 30–36.
 - [21] For simplicity, we assume the same numerical value for both the relative and absolute tolerance. The algorithm will always match the most stringent of the two requirements.
 - [22] S. Gariazzo, C. Giunti, M. Laveder, and Y. F. Li, *Model-Independent $\bar{\nu}_e$ Short-Baseline Oscillations from Reactor Spectral Ratios*, *Phys.Lett.B* **782** (2018) 13–21, [[arXiv:1801.06467](#)].
 - [23] J. J. Bennett et al., *in preparation*, .
 - [24] P. F. de Salas, D. V. Forero, C. A. Ternes, M. Tórtola, and J. W. F. Valle, *Status of neutrino oscillations 2018: 3 σ hint for normal mass ordering and improved CP sensitivity*, *Phys. Lett. B* **782** (jul, 2018) 633–640, [[arXiv:1708.01186](#)].
 - [25] M. Tanabashi et al., *Review of Particle Physics*, *Phys.Rev.* **D98** (2018) 030001.